

## Electronic Supplementary Information

### **A new type pyranthrene-based copolymer as a promising hole-transport material for perovskite solar cells**

Azat F. Akbulatov,<sup>a</sup> Ekaterina A. Khakina,<sup>b</sup> Nikita A. Emelianov,<sup>a</sup> Olga A. Kraevaya,<sup>a</sup> Lyubov A. Frolova,<sup>a</sup> and Pavel A. Troshin<sup>c,a</sup>

<sup>a</sup> Federal Research Center of Problems of Chemical Physics and Medicinal Chemistry of the Russian Academy of Sciences, Semenov Prospect 1, Chernogolovka, 142432, Russia

<sup>b</sup> A. N. Nesmeyanov Institute of Organoelement Compounds of the Russian Academy of Sciences, Vavilov Str. 28, 119991 Moscow, Russia

<sup>c</sup> Zhengzhou Research Institute of HIT, 26 Longyuan East 7th, Jinshui District, Zhengzhou, Henan Province, 450000, China

#### AUTHOR INFORMATION

#### **Corresponding Author**

E-mail: [qweas89@mail.ru](mailto:qweas89@mail.ru), Tel: +7-496-522-1937

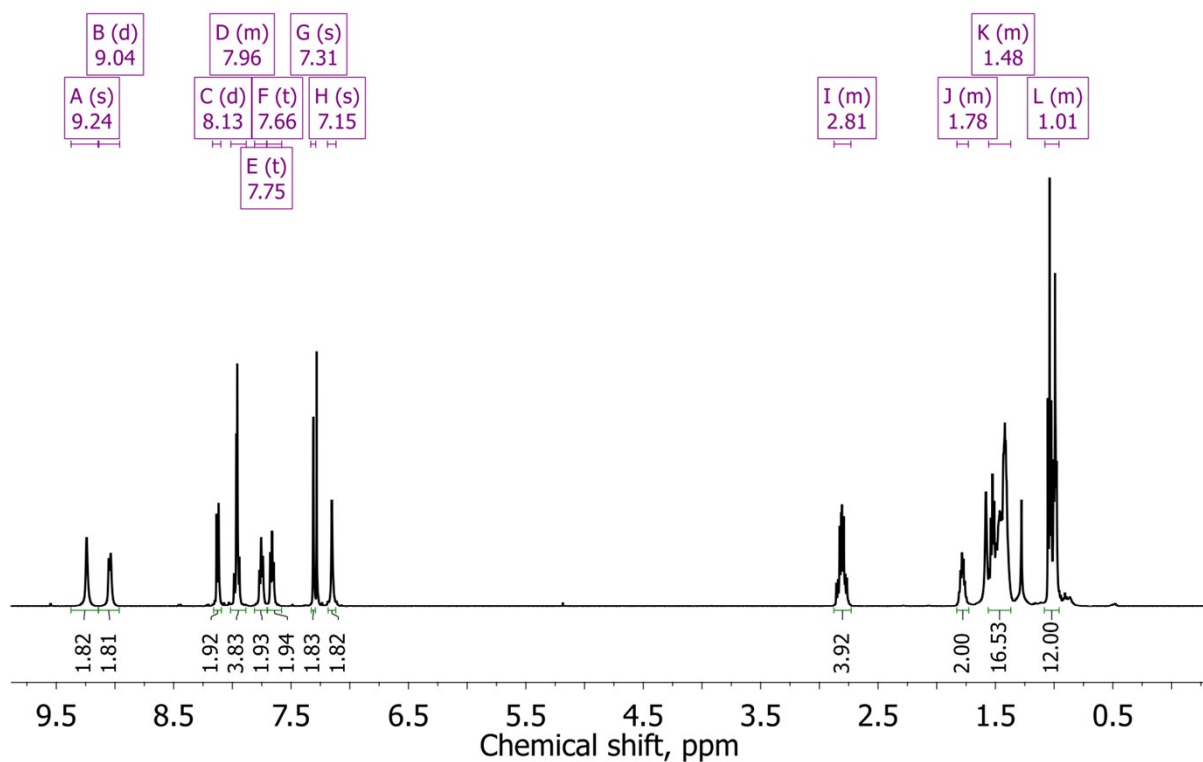


Figure S1.  $^1\text{H}$  NMR spectrum of compound **2** (solvent –  $\text{CDCl}_3$ ).

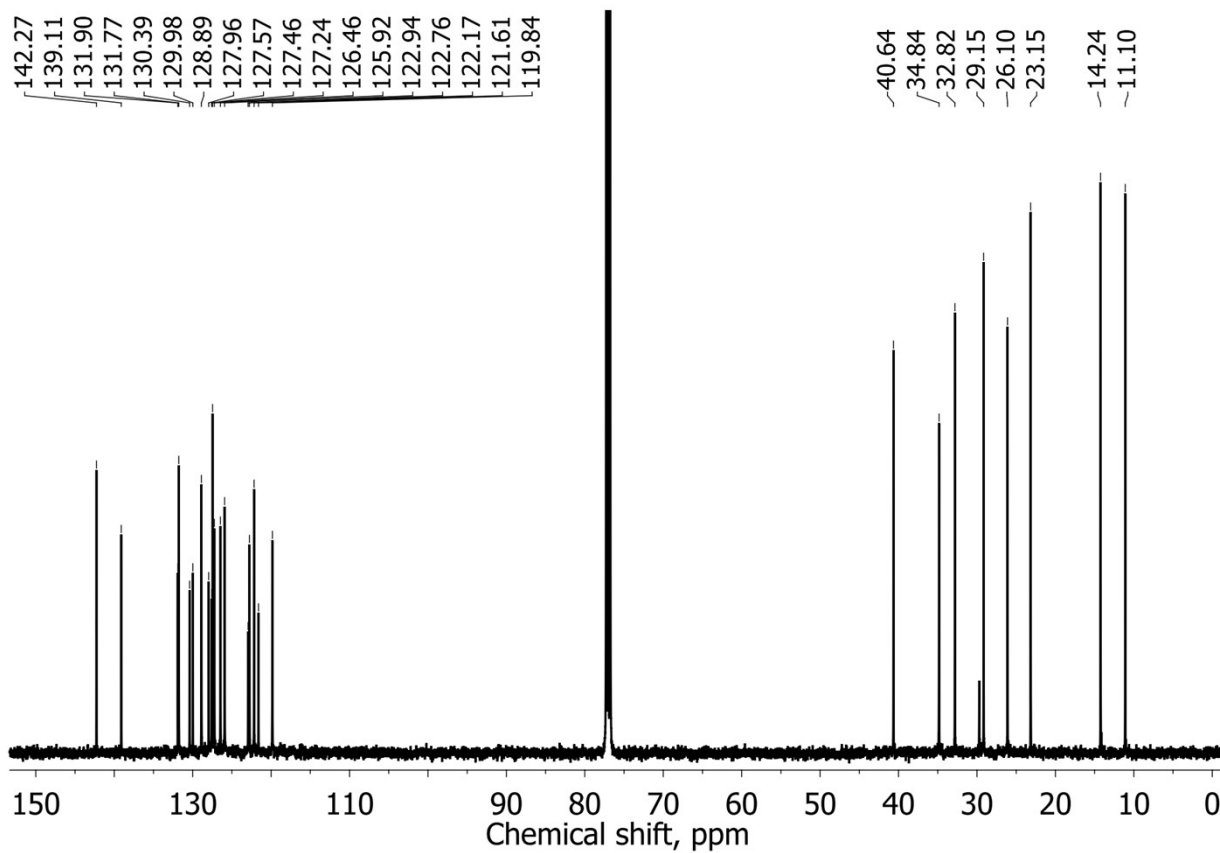


Figure S2.  $^{13}\text{C}$  NMR spectrum of compound **2** (solvent –  $\text{CDCl}_3$ ).

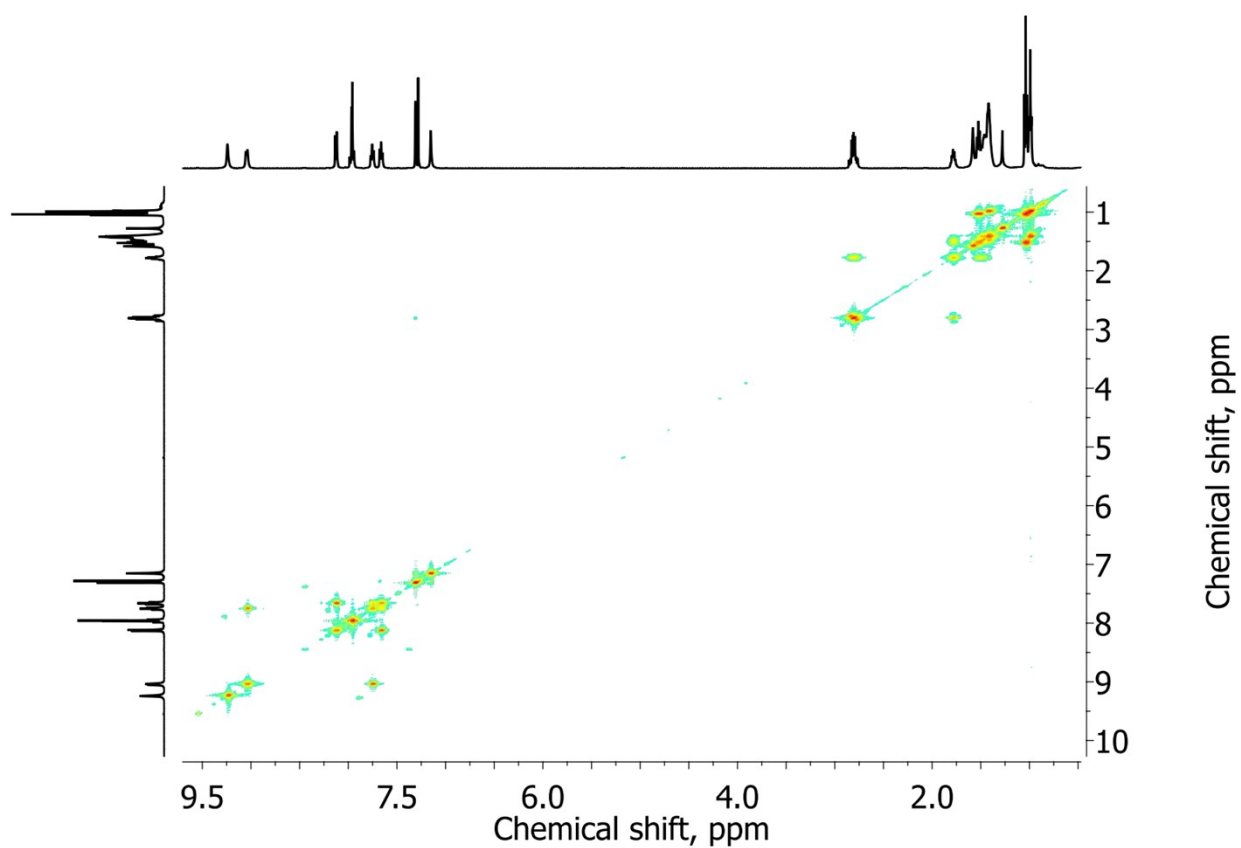


Figure S3.  $^1\text{H}$ - $^1\text{H}$  COSY NMR spectrum of compound **2** (solvent –  $\text{CDCl}_3$ ).

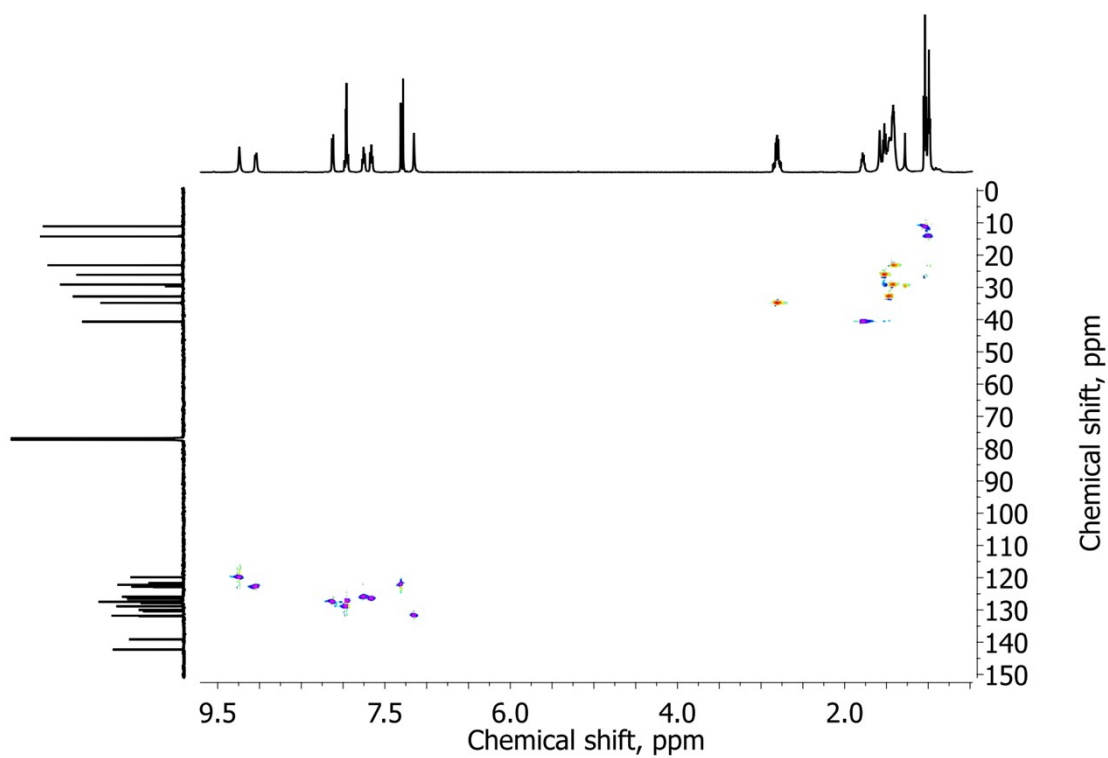


Figure S4.  $^1\text{H}$ - $^{13}\text{C}$  HSQC NMR spectrum of compound **2** (solvent –  $\text{CDCl}_3$ ).

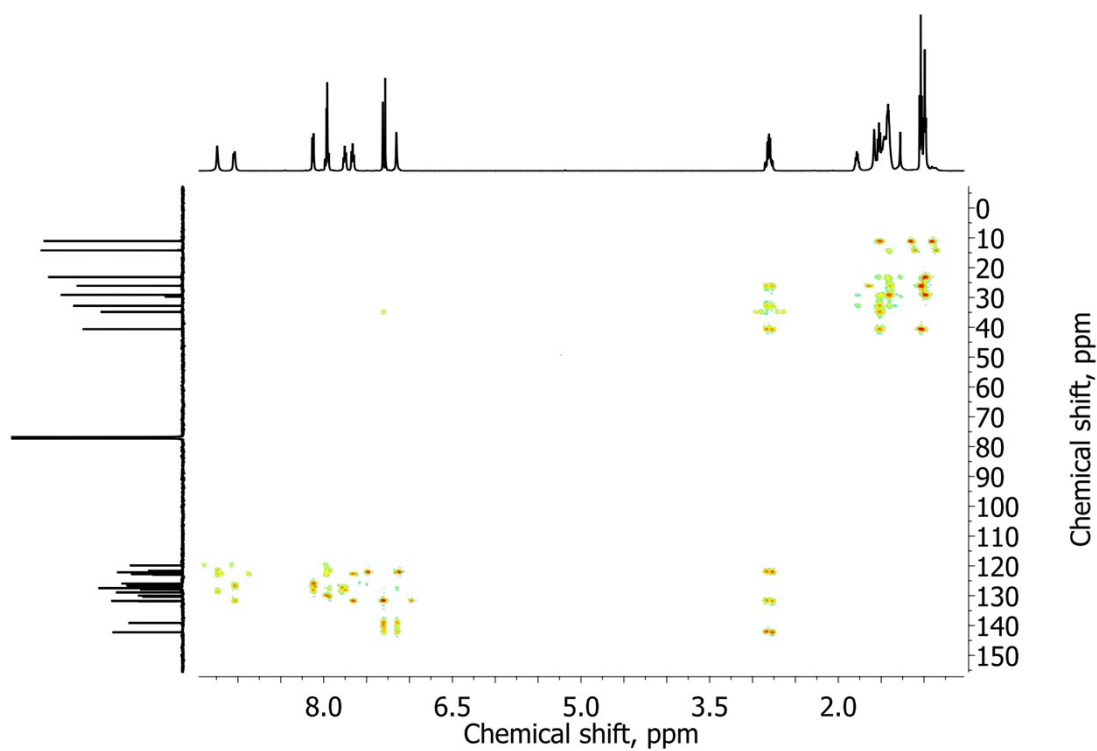


Figure S5.  $^1\text{H}$ - $^{13}\text{C}$  HMBC NMR spectrum of compound **2** (solvent –  $\text{CDCl}_3$ ).

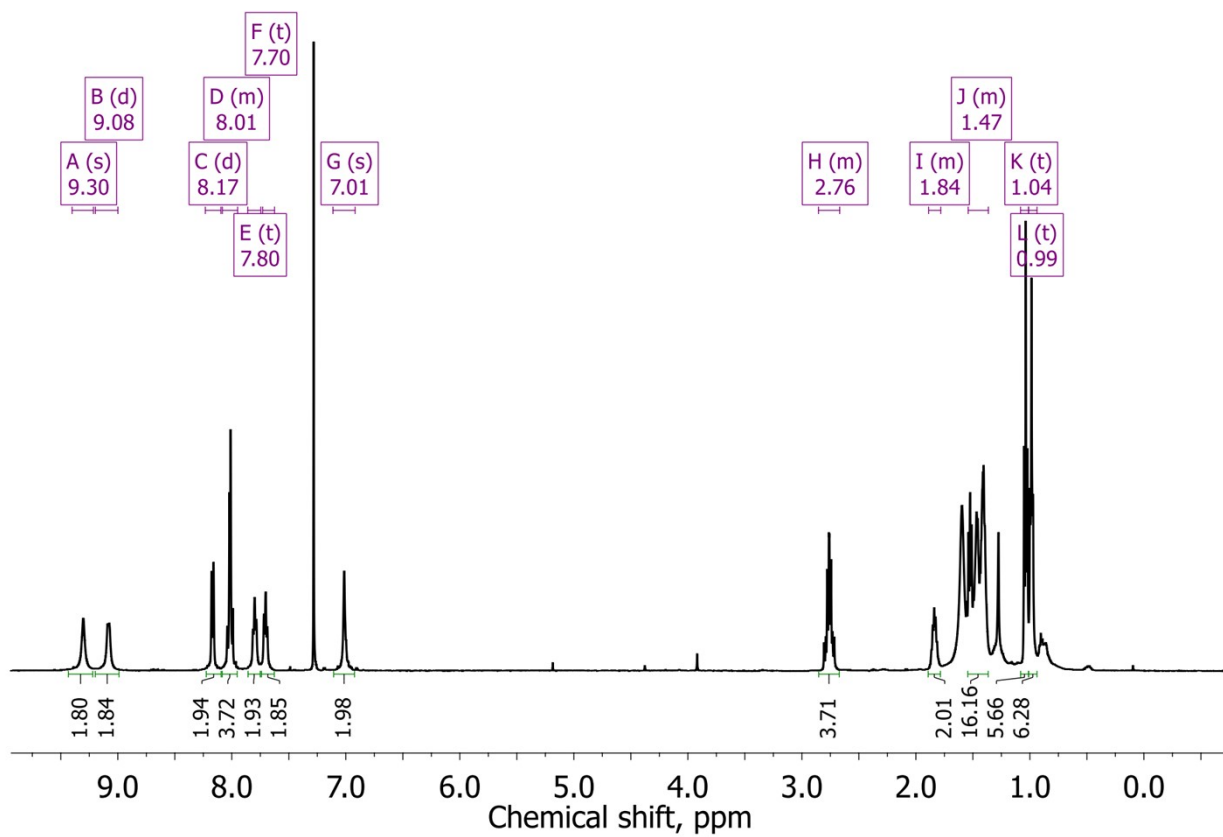


Figure S6.  $^1\text{H}$  NMR spectrum of compound **3** (solvent –  $\text{CDCl}_3$ ).

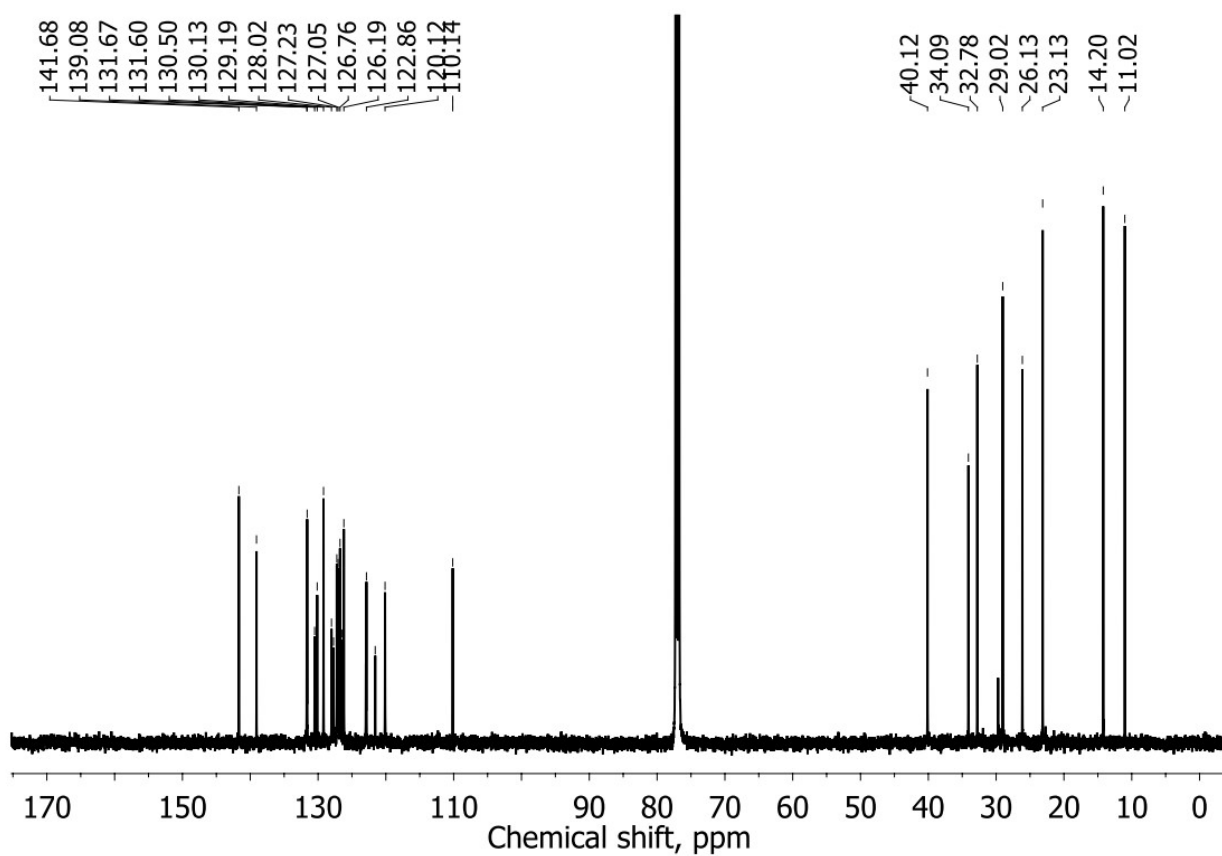


Figure S7.  $^{13}\text{C}$  NMR spectrum of compound **3** (solvent –  $\text{CDCl}_3$ ).

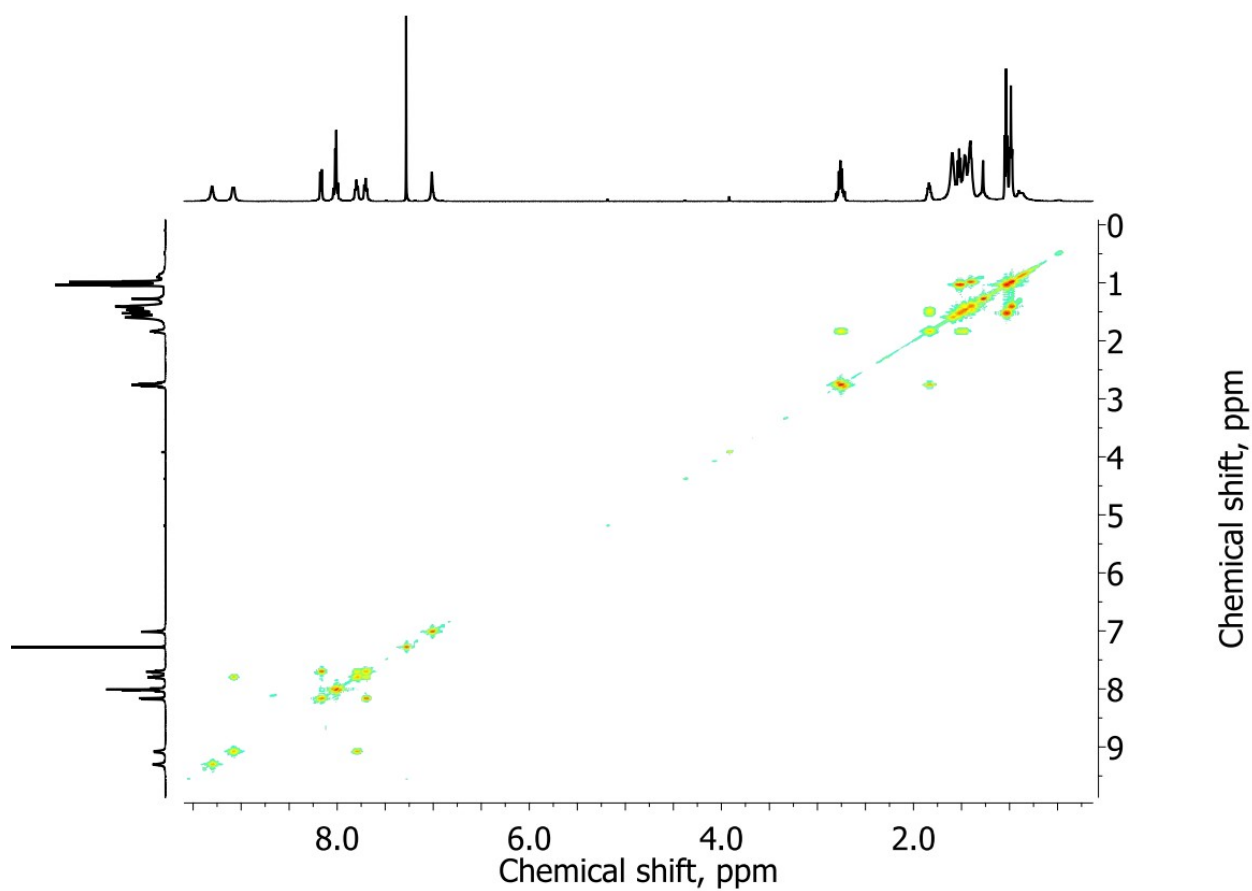


Figure S8.  $^1\text{H}$ - $^1\text{H}$  COSY NMR spectrum of compound **3** (solvent –  $\text{CDCl}_3$ ).

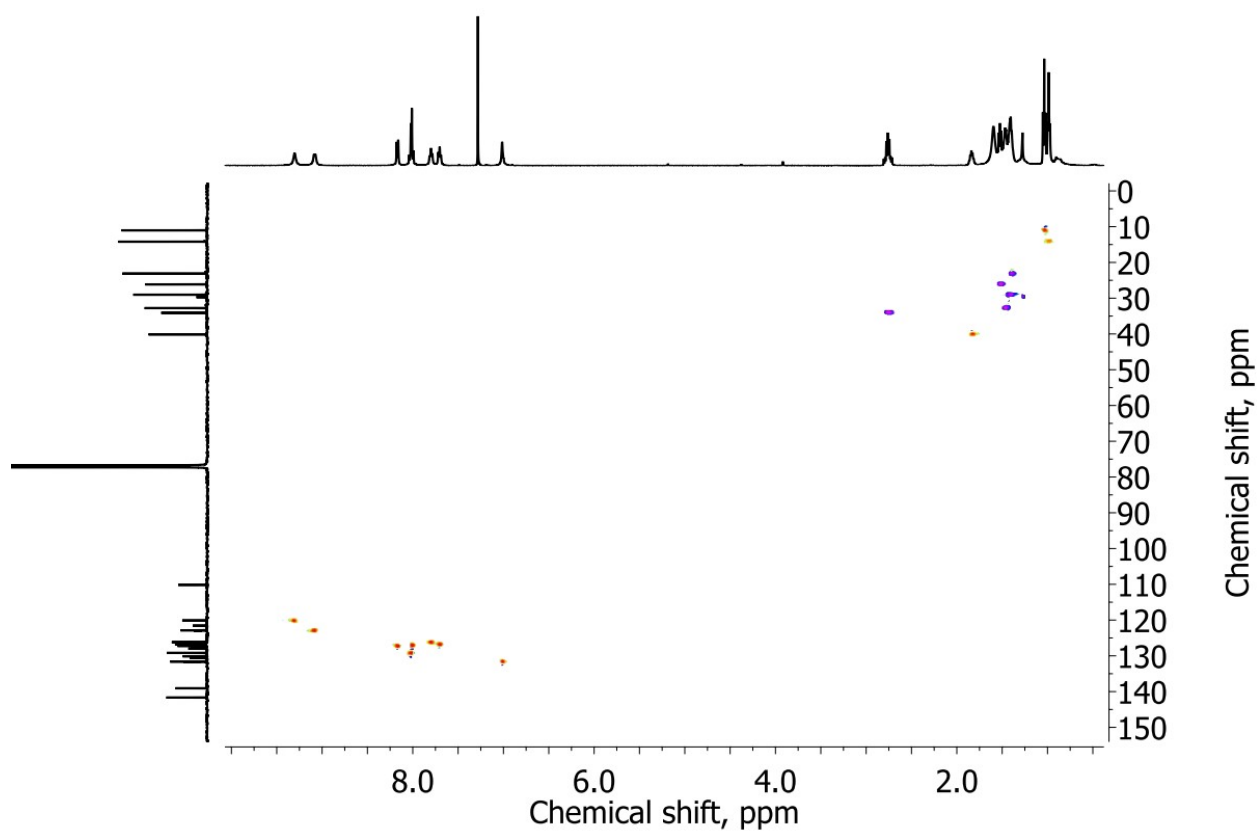


Figure S9.  $^1\text{H}$ - $^{13}\text{C}$  HSQC NMR spectrum of compound **3** (solvent –  $\text{CDCl}_3$ ).

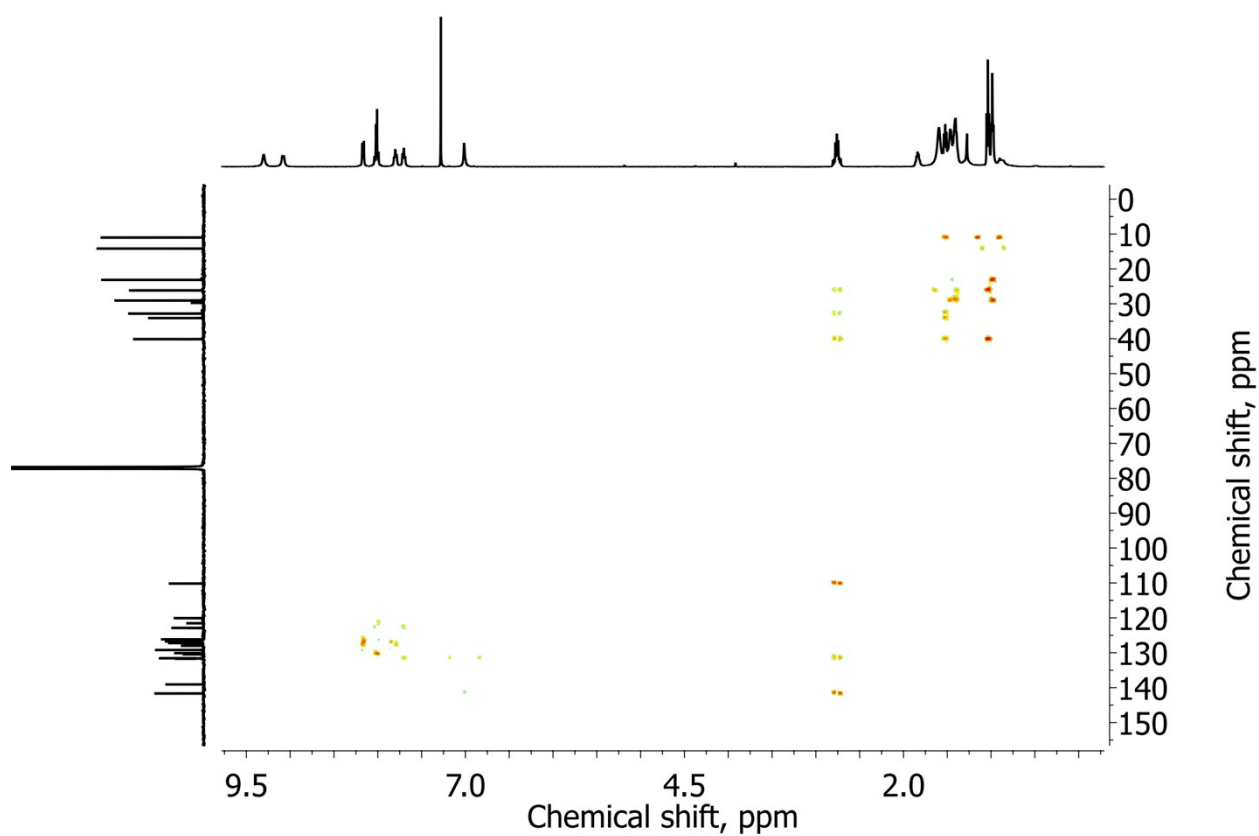


Figure S10.  $^1\text{H}$ - $^{13}\text{C}$  HMBC NMR spectrum of compound **3** (solvent –  $\text{CDCl}_3$ ).

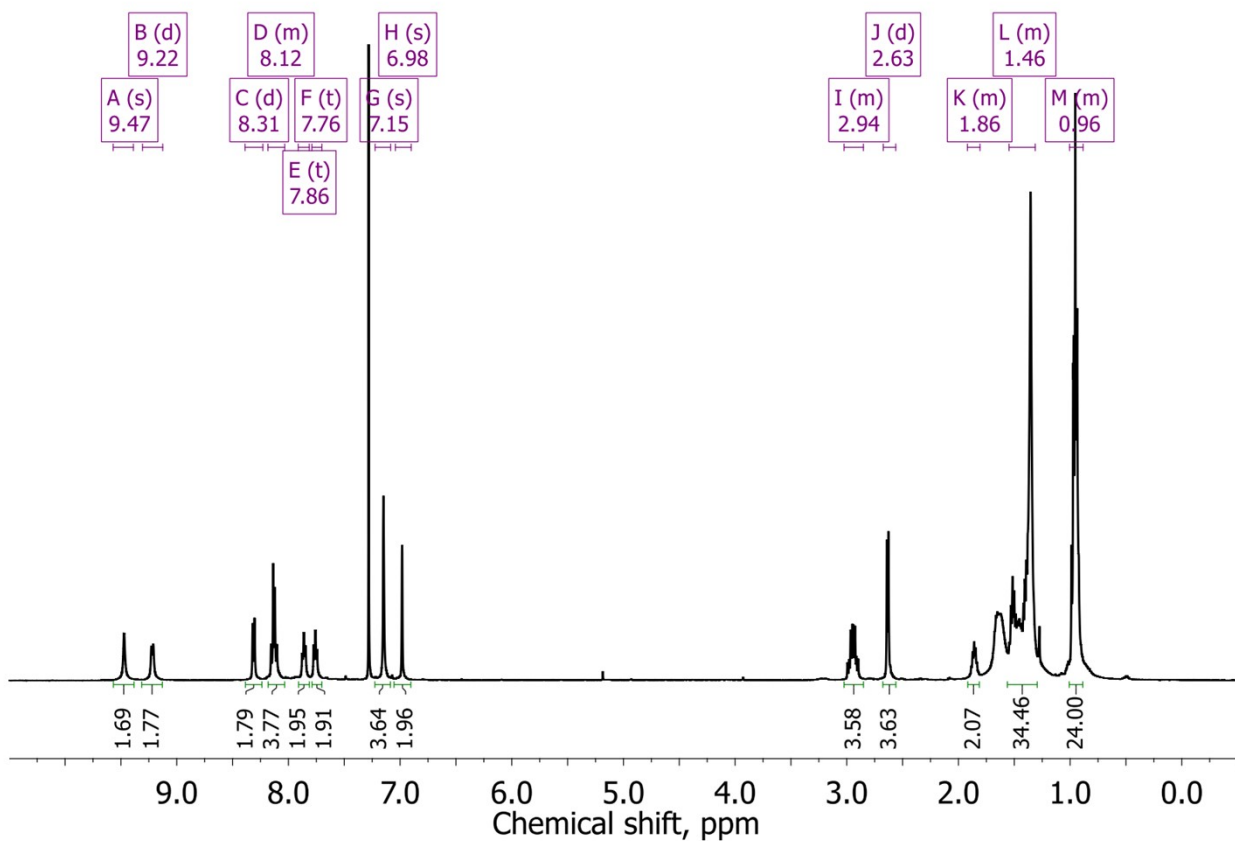


Figure S11.  $^1\text{H}$  NMR spectrum of compound **5** (solvent –  $\text{CDCl}_3$ ).

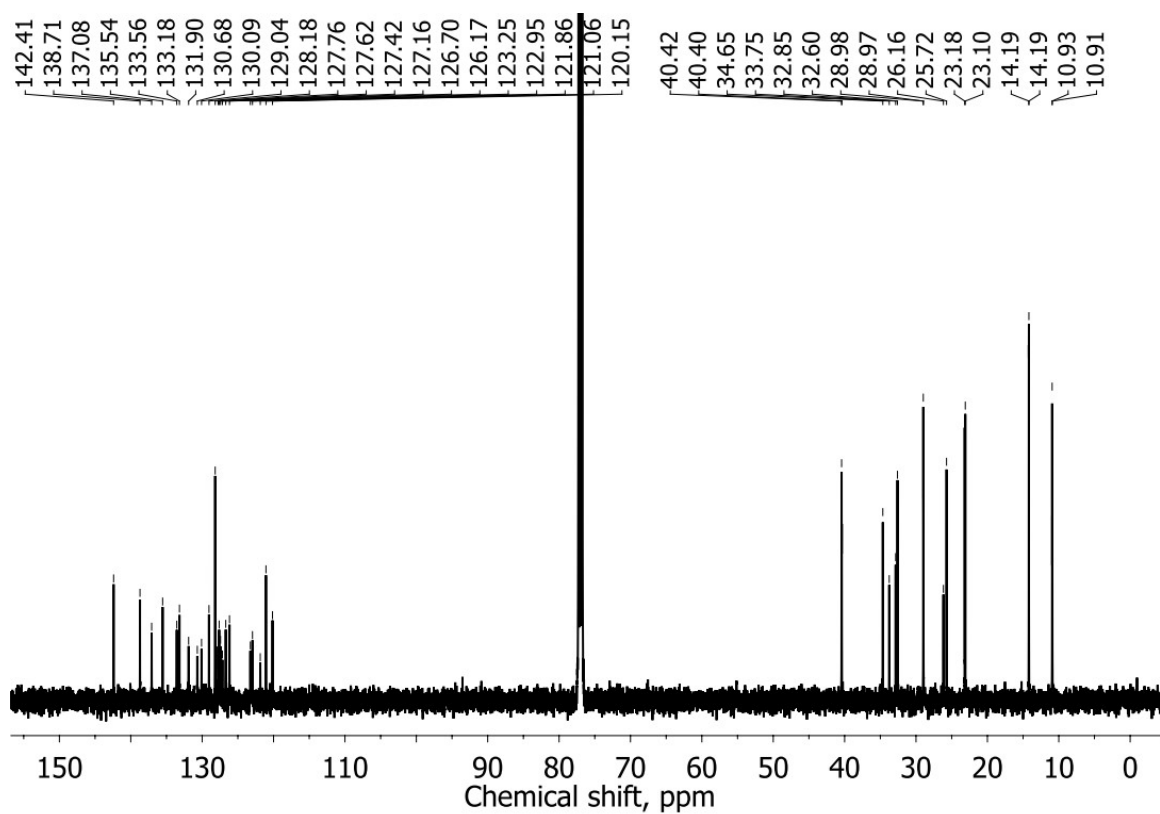


Figure 12.  $^{13}\text{C}$  NMR spectrum of compound **5** (solvent –  $\text{CDCl}_3$ ).

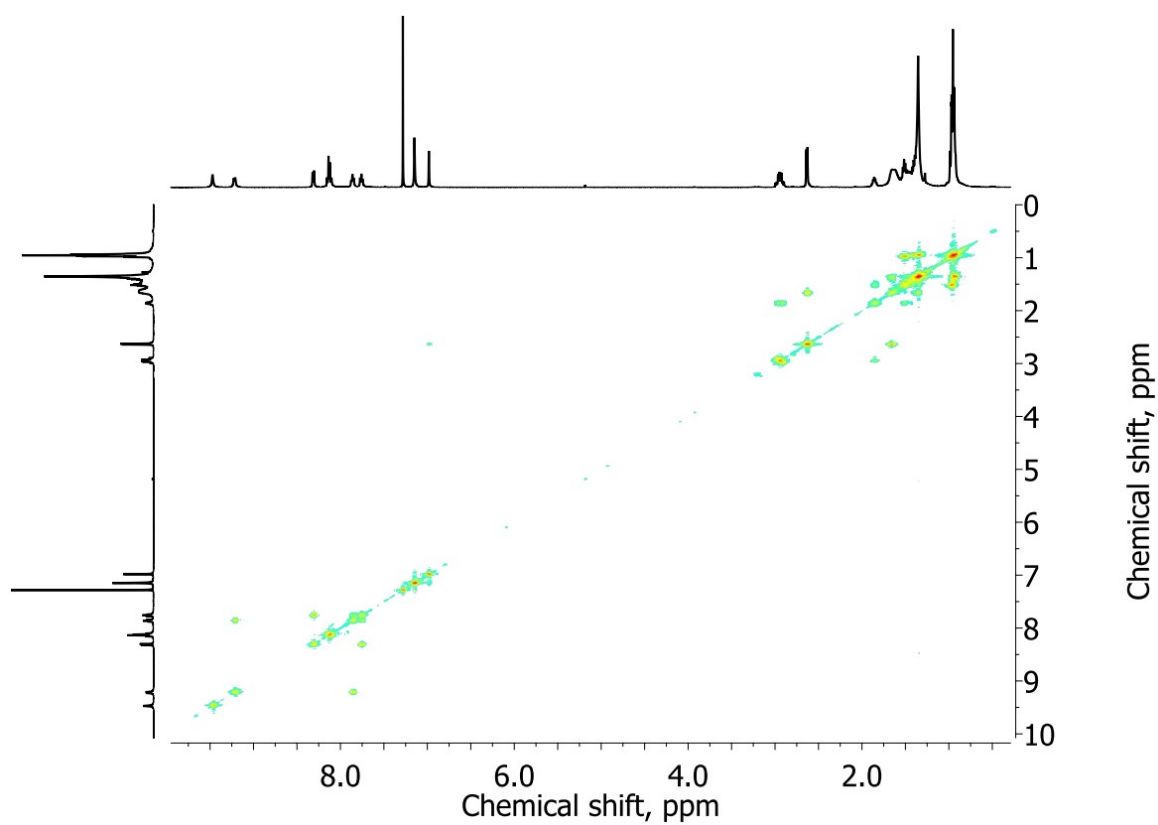


Figure S13. <sup>1</sup>H-<sup>1</sup>H COSY NMR spectrum of compound **5** (solvent – CDCl<sub>3</sub>).

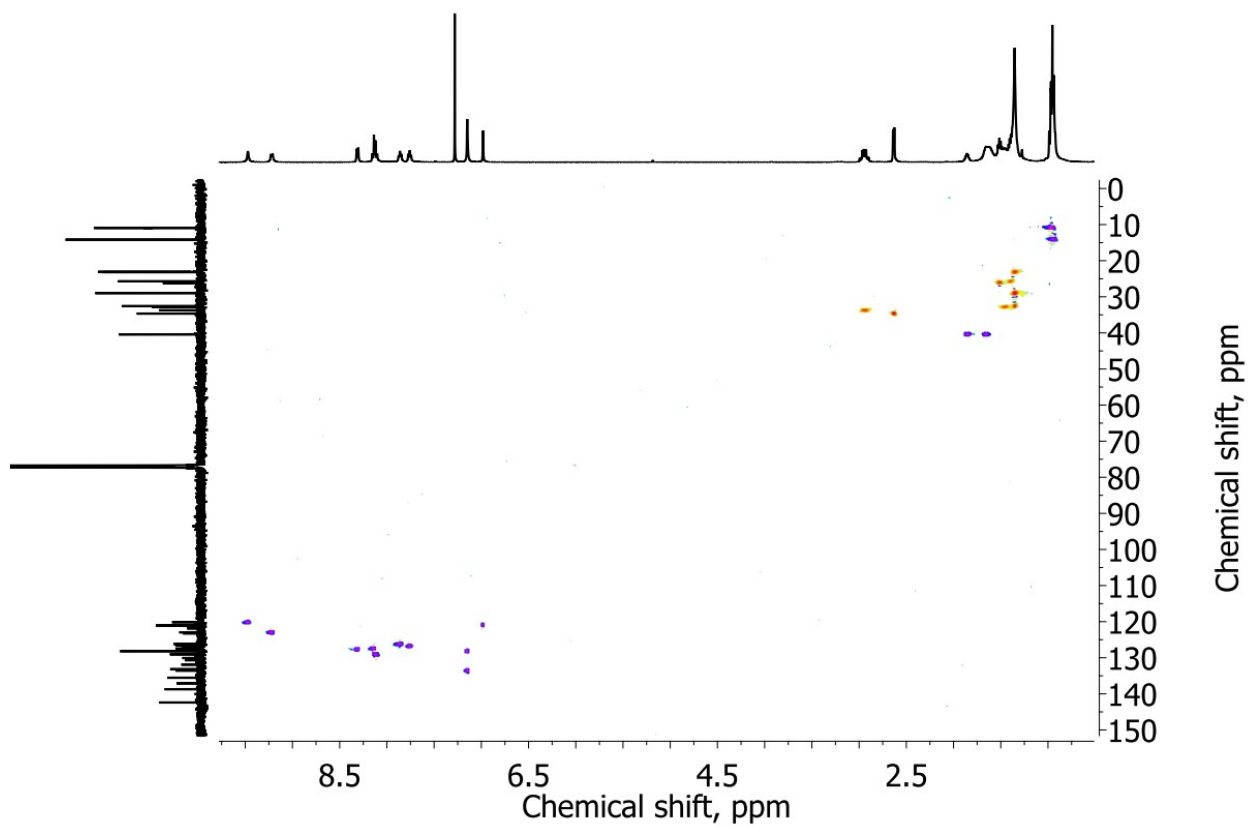


Figure S14. <sup>1</sup>H-<sup>13</sup>C HSQC NMR spectrum of compound **5** (solvent – CDCl<sub>3</sub>).



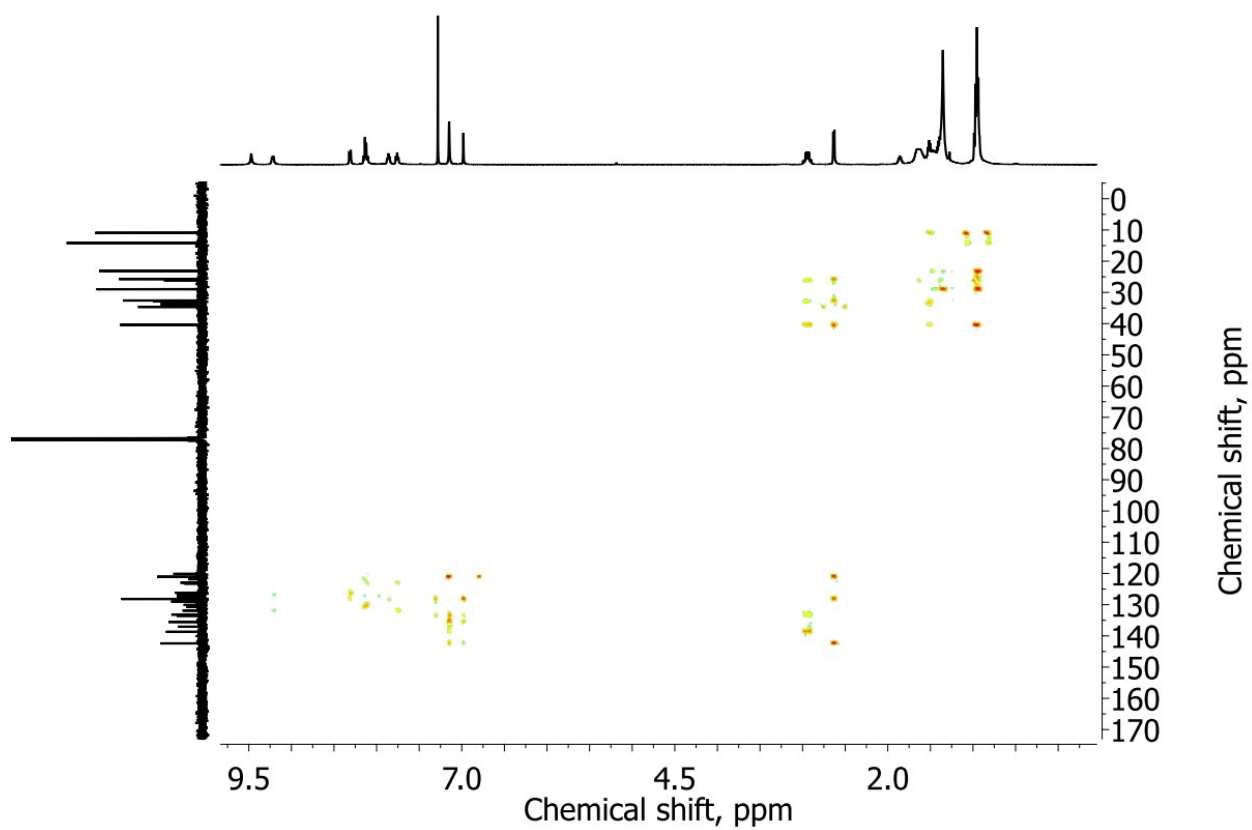


Figure S15.  $^1\text{H}$ - $^{13}\text{C}$  HMBC NMR spectrum of compound **5** (solvent –  $\text{CDCl}_3$ ).

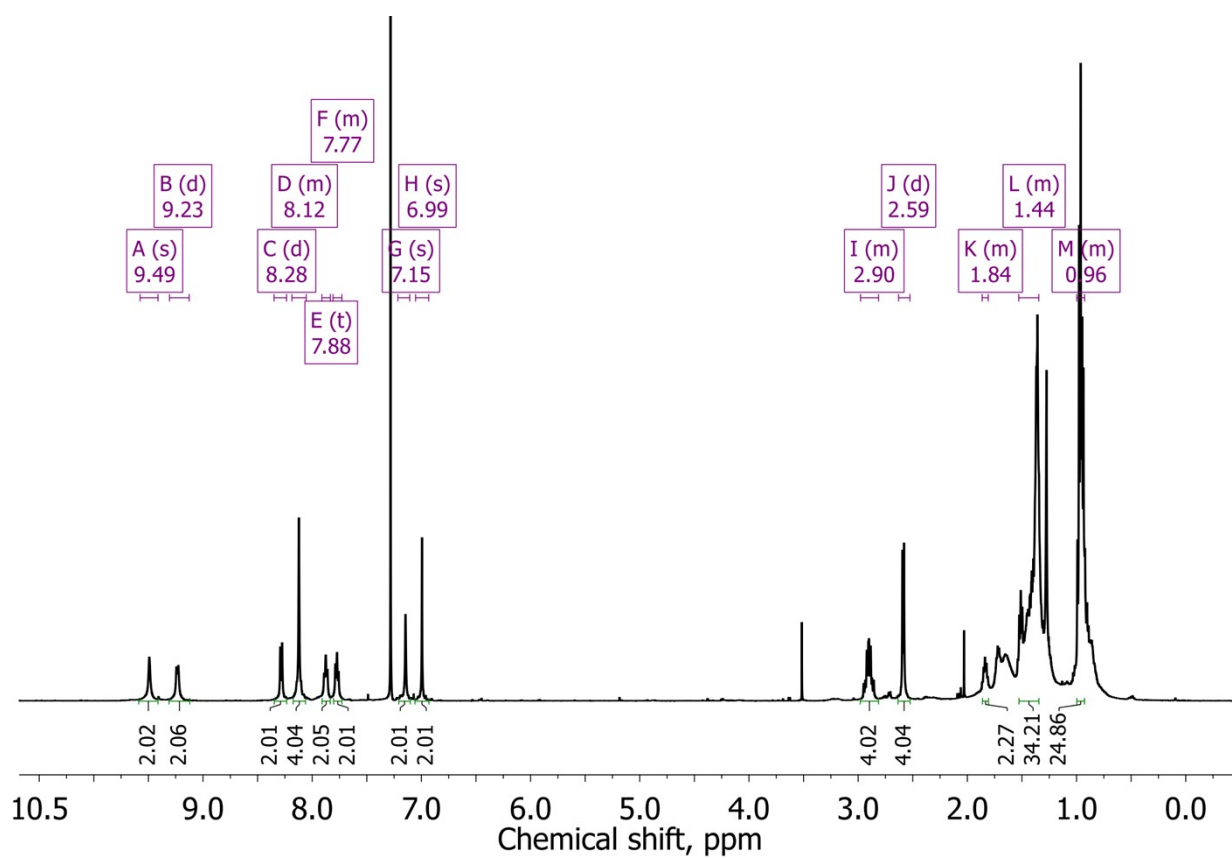


Figure S16.  $^1\text{H}$  NMR spectrum of compound **6** (solvent –  $\text{CDCl}_3$ ).

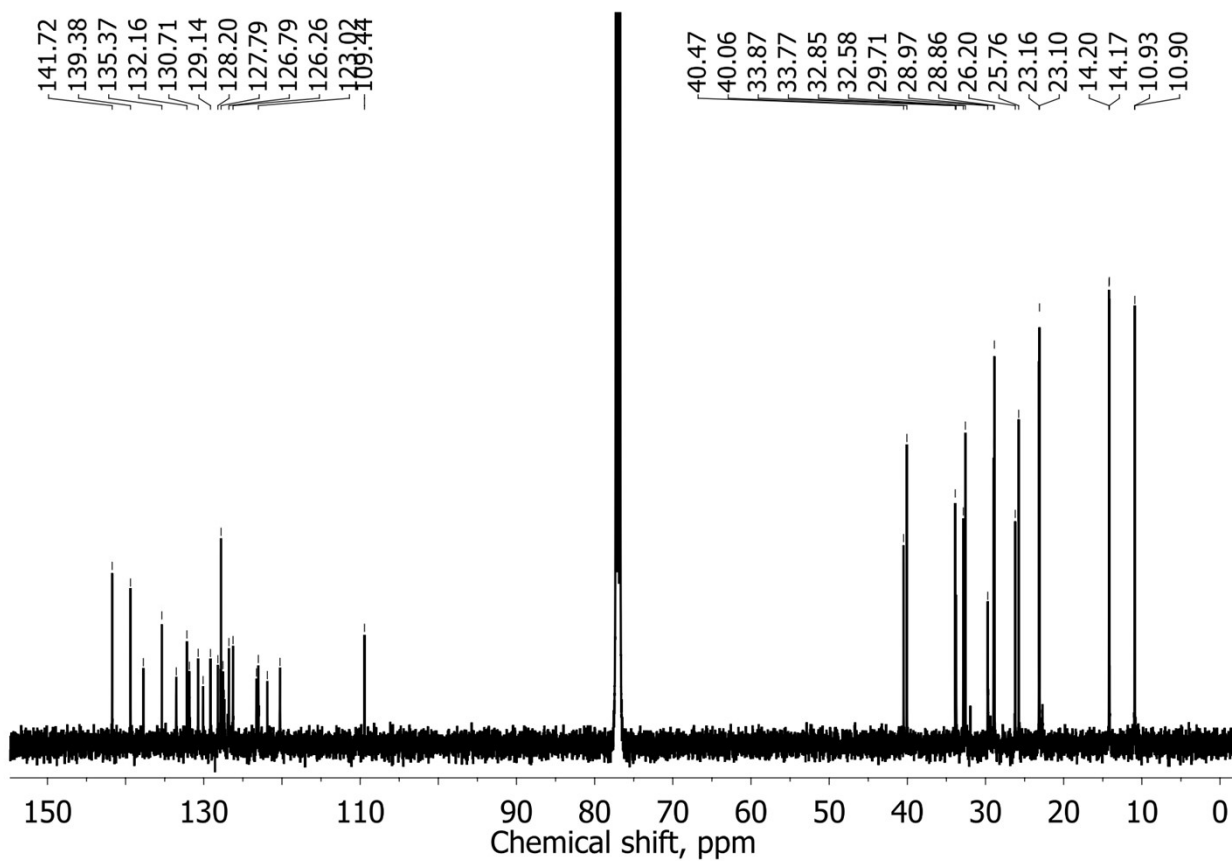


Figure 17.  $^{13}\text{C}$  NMR spectrum of compound **6** (solvent –  $\text{CDCl}_3$ ).

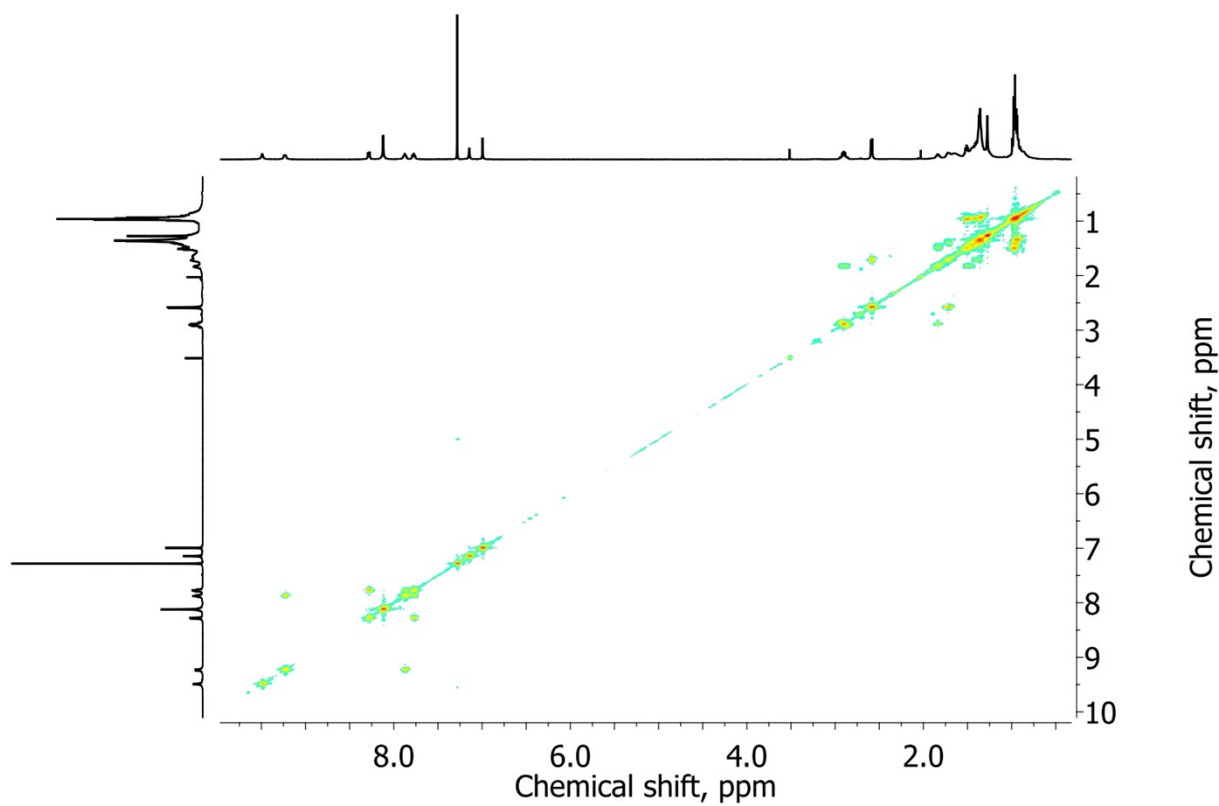


Figure S18.  $^1\text{H}$ - $^1\text{H}$  COSY NMR spectrum of compound **6** (solvent –  $\text{CDCl}_3$ ).

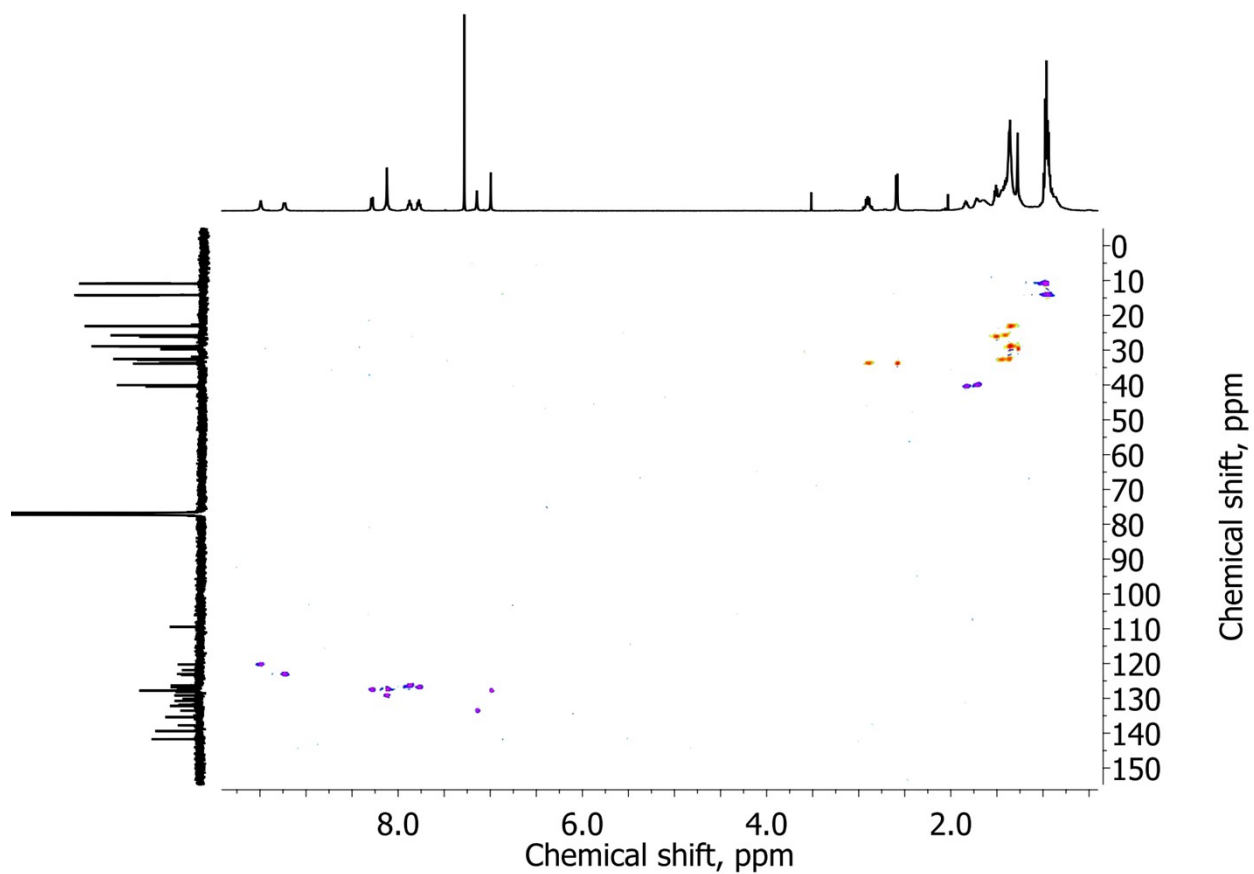


Figure S19.  $^1\text{H}$ - $^{13}\text{C}$  HSQC NMR spectrum of compound **6** (solvent –  $\text{CDCl}_3$ ).

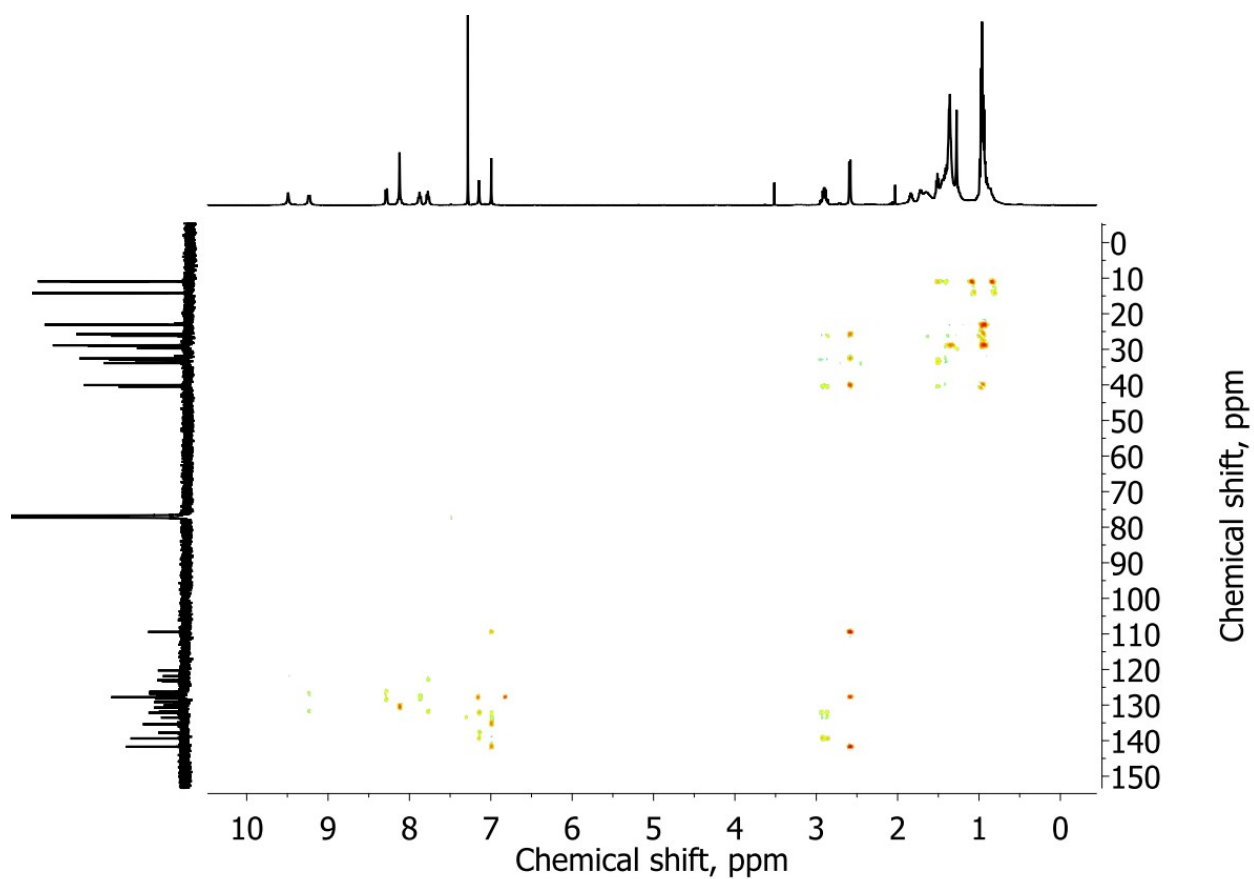


Figure S20.  $^1\text{H}$ - $^{13}\text{C}$  HMBC NMR spectrum of compound **6** (solvent –  $\text{CDCl}_3$ ).

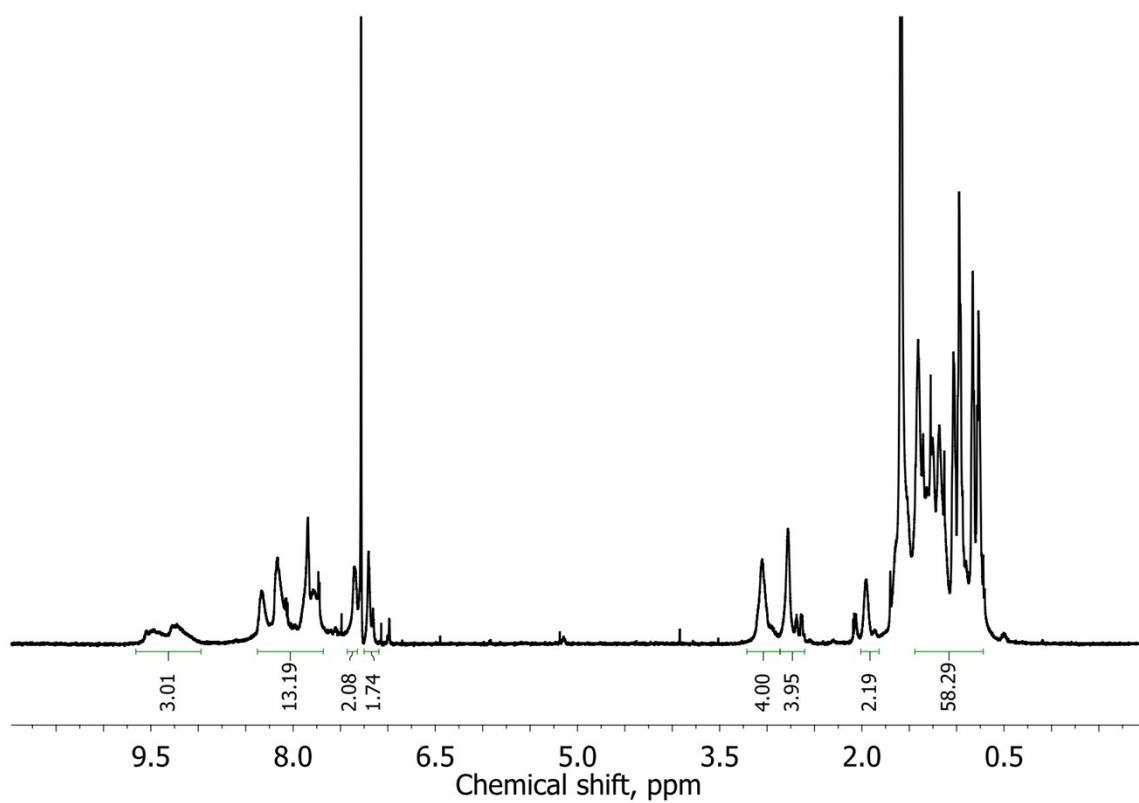


Figure S21.  $^1\text{H}$  NMR spectrum of compound **PATTBTT** (solvent –  $\text{CDCl}_3$ ).

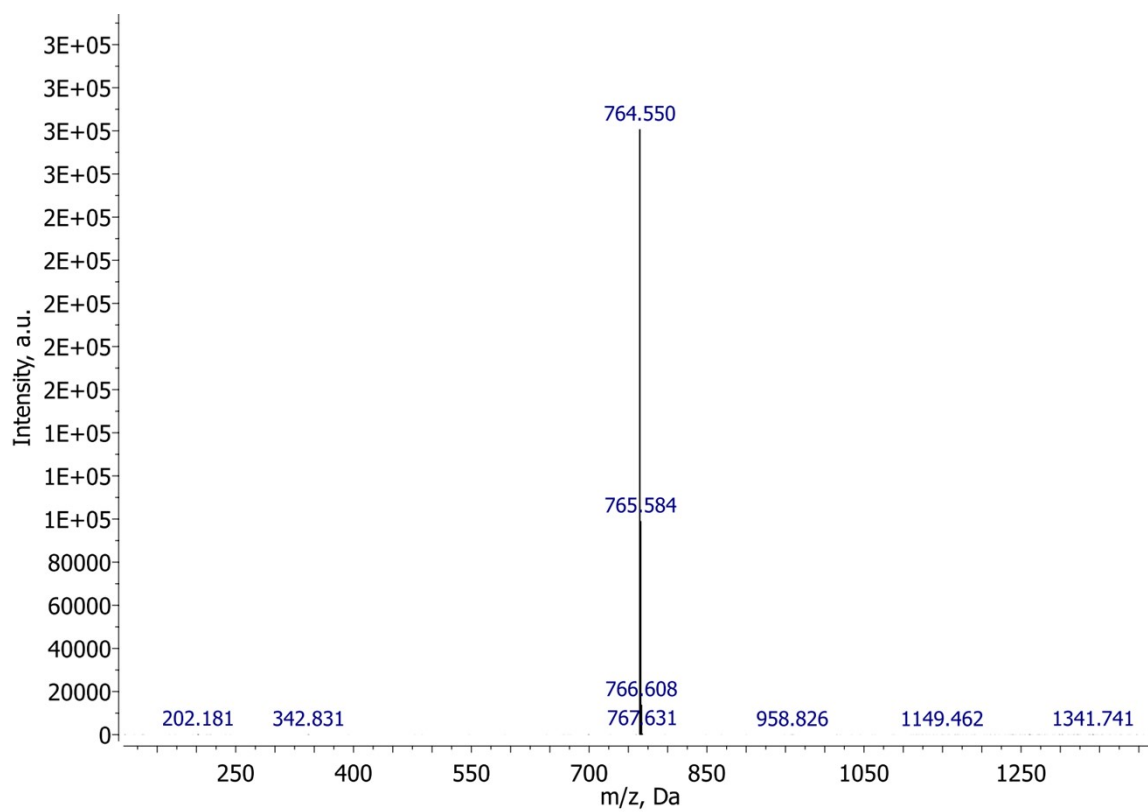


Figure S22. MALDI mass spectrum of compound **2**

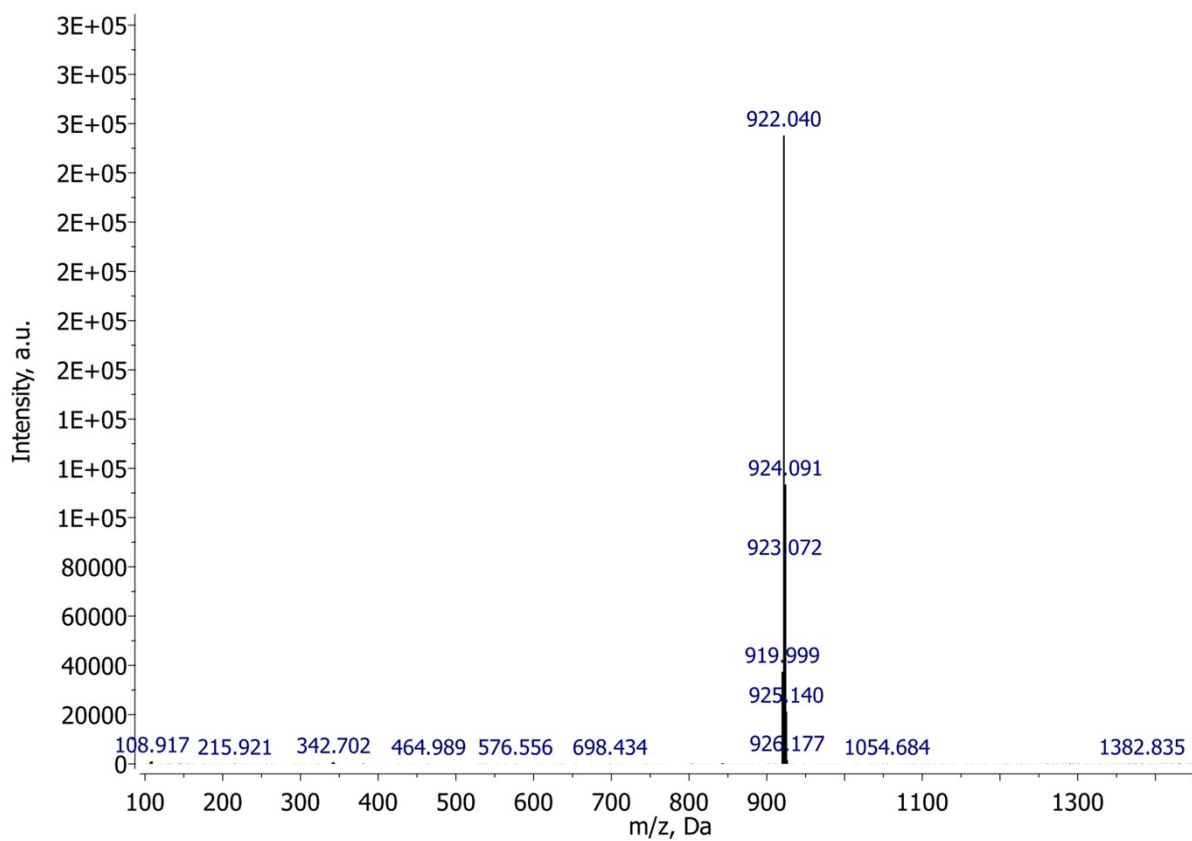


Figure S23. MALDI mass spectrum of compound **3**

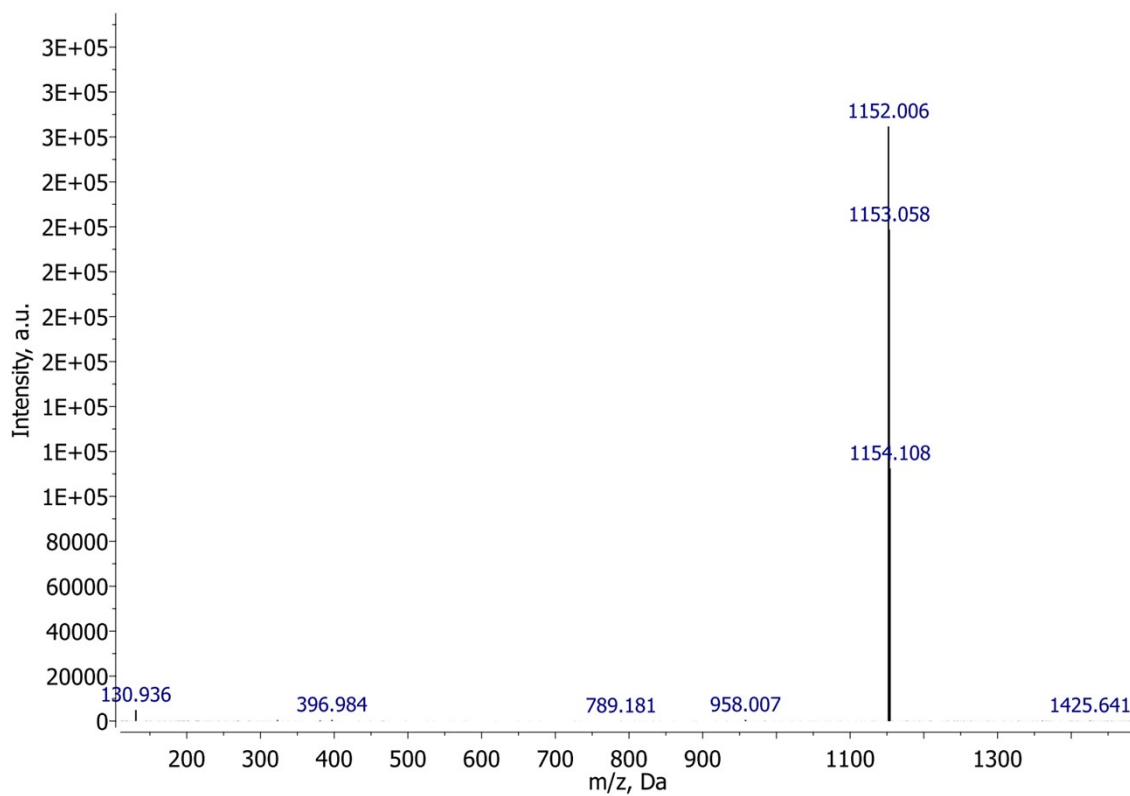


Figure S24. MALDI mass spectrum of compound **5**

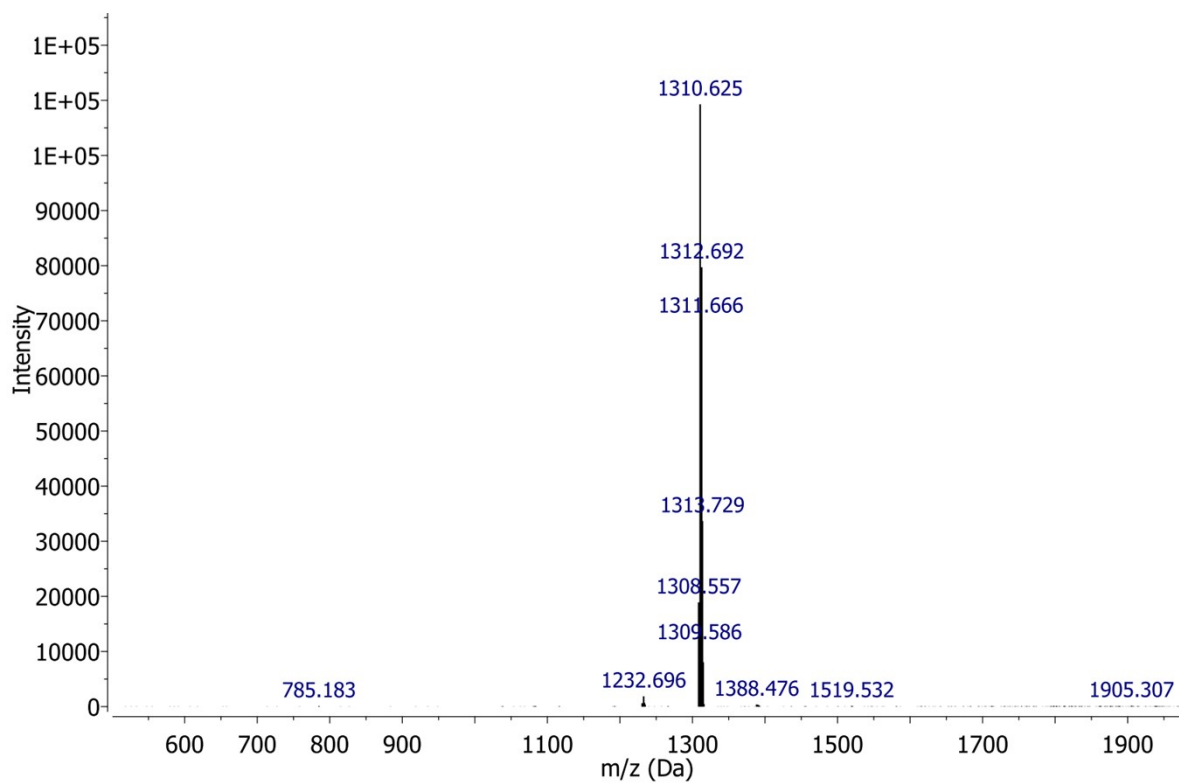


Figure S25. MALDI mass spectrum of compound **6**

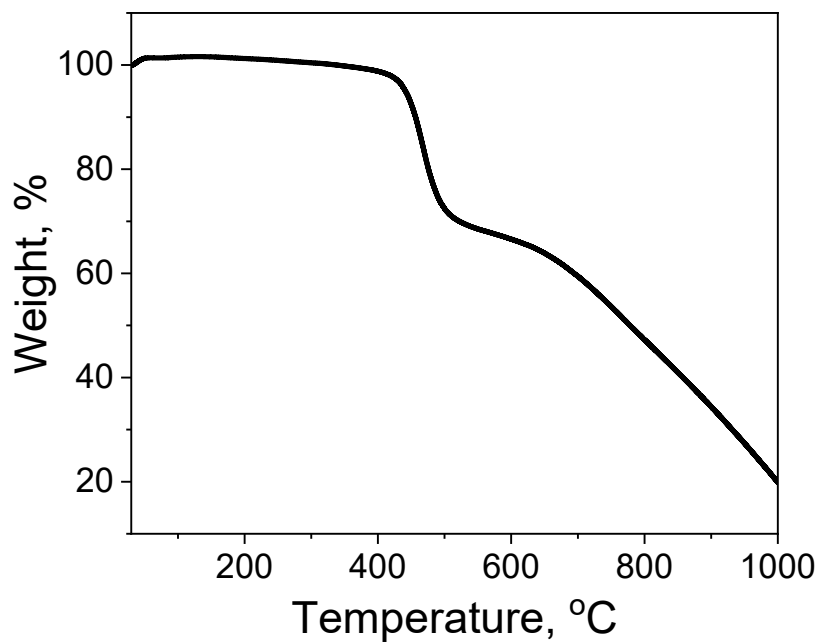


Figure S26. Results of thermogravimetric analysis of the polymer **PATTBTT**

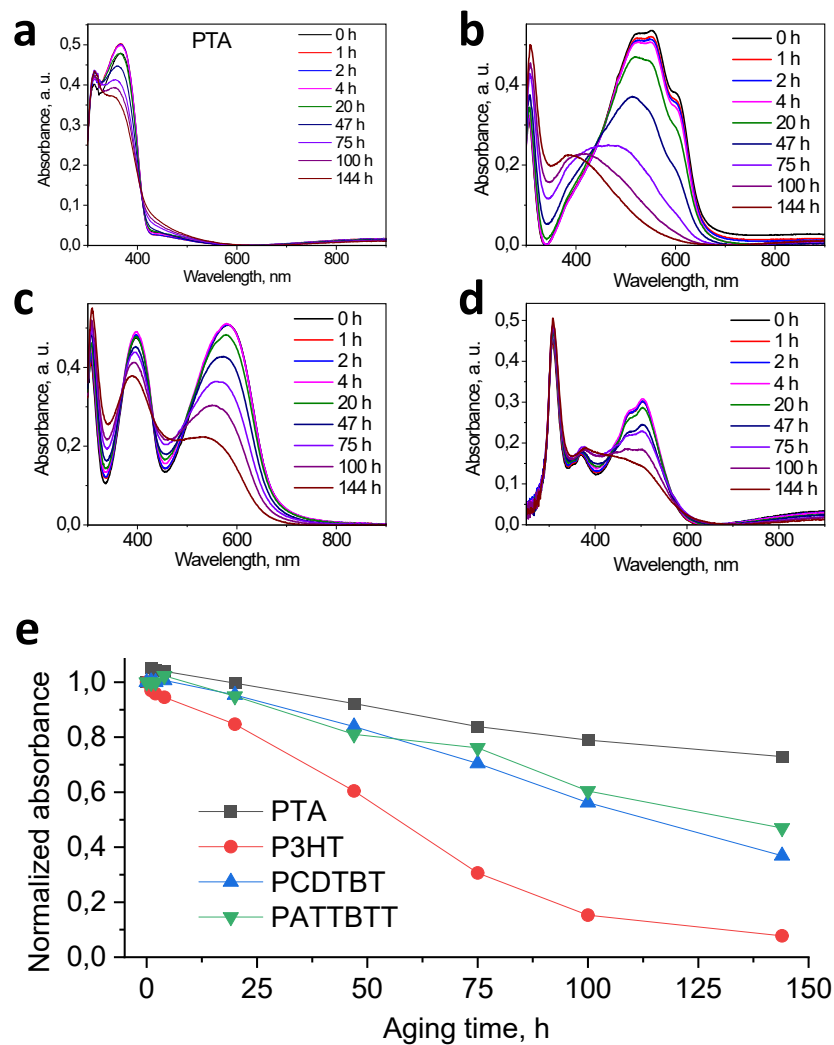


Figure S27. The evolution of the normalized UV-vis absorption spectra of thin films of PTA (a), P3HT (b), PCDTBT (c), and PATTBTT (d) upon aging under UV light exposure. The aging profiles of all studied polymers plotted as the evolution of the maximal film absorbance vs aging time (e).

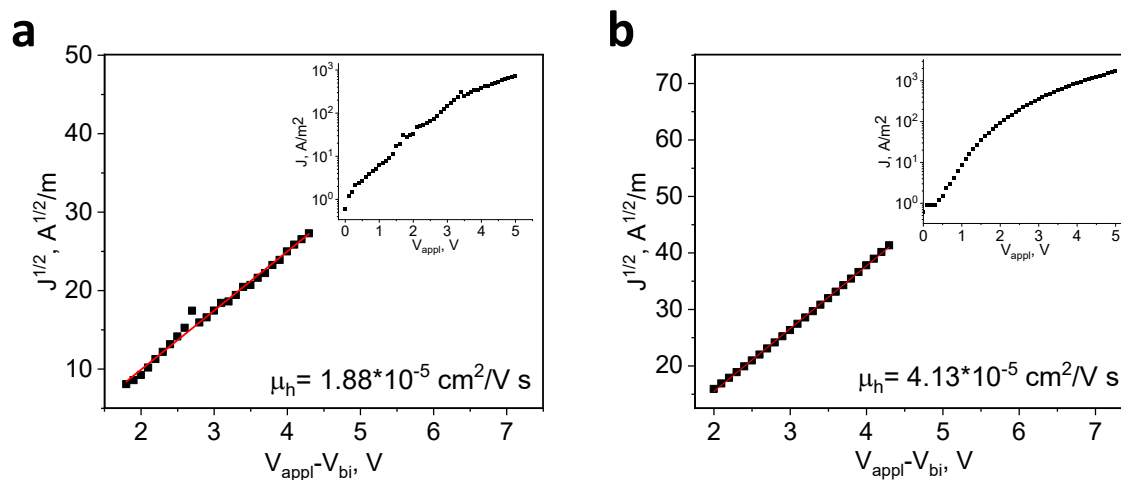


Figure S28. Current density vs. voltage curves, measured in ITO/PEDOT:PSS/PTA/V<sub>2</sub>O<sub>5</sub>/Al (a) and ITO/PEDOT:PSS/PATTBTT/V<sub>2</sub>O<sub>5</sub>/Al (b) diodes.

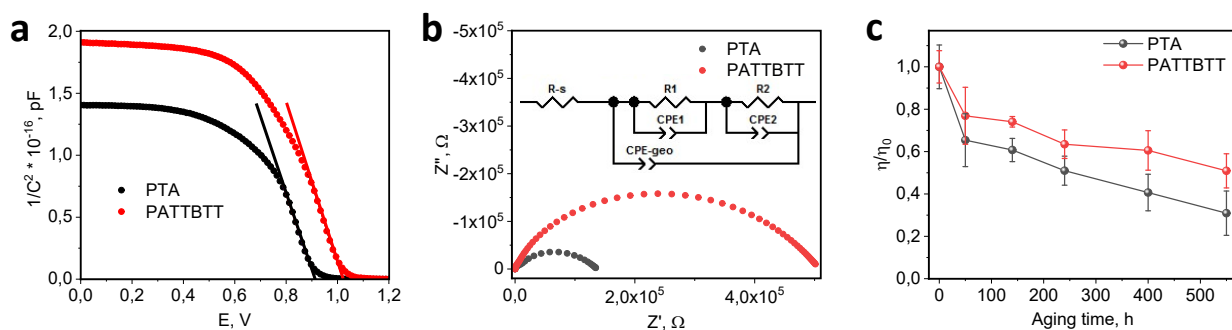


Figure S29. Capacitance-voltage characteristics (a) and Nyquist plots (b) of devices assembled using PTA and PATTBTT as HTL materials. Evolution of PCE of PSCs with PTA and PATTBTT under constant white-light illumination ( $P=80 \text{ mW/cm}^2$ ,  $40^\circ\text{C}$ ) (c).

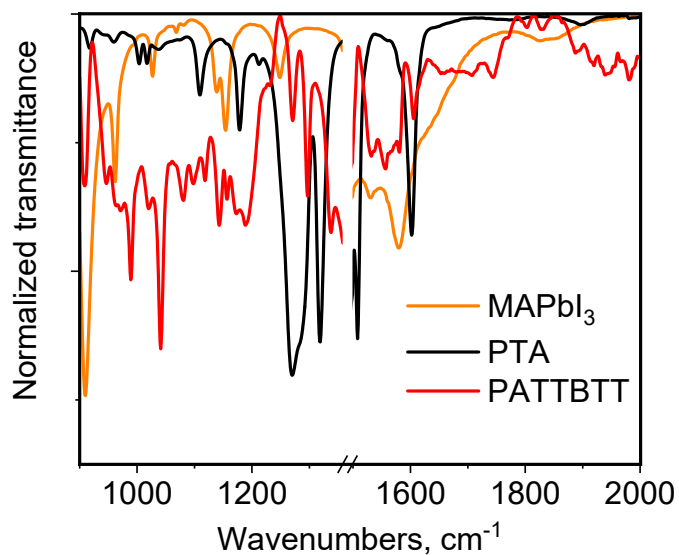


Figure S30. ATR FTIR spectra of MAPbI<sub>3</sub>, PTA and PATTBTT.